

Second-order mixed-moment model with differentiable ansatz function in slab geometry

Florian Schneider^a

^a*Fachbereich Mathematik, TU Kaiserslautern, Erwin-Schrödinger-Str., 67663 Kaiserslautern, Germany,
schneider@mathematik.uni-kl.de*

Abstract

We study differentiable mixed-moment models (full zeroth and first moment, half higher moments) for a Fokker-Planck equation in one space dimension. Mixed-moment minimum-entropy models are known to overcome the zero net-flux problem of full-moment minimum entropy M_N models. Realizability theory for these modification of mixed moments is derived for second order. Numerical tests are performed with a kinetic first-order finite volume scheme and compared with M_N , classical MM_N and a P_N reference scheme.

Keywords: moment models, minimum entropy, Fokker-Planck equation, realizability

2010 MSC: 35L40, 35Q84, 65M08, 65M70

1. Introduction

We investigate time-dependent kinetic transport equations like the Fokker–Planck equation, arising from the Boltzmann equation [3, 6] under the assumption of extremely forward-peaked scattering [30]. They describe the propagation of “radiation particles” like photons or electrons which travel at time t from their current position in a specific direction and how they interact with the surrounding matter. Without any assumptions or dimensional reductions this typically leads to a six- or seven-dimensional state space. Applications reach from electron transport in solids and plasmas, neutron transport in nuclear reactors, photon transport in superfluids and radiative transfer to the context of biological modelling, e.g. for studying cell movement (chemotaxis/haptotaxis) or wolf migration [7, 18, 21].

A common approach to reduce the dimensionality is given by the method of moments [12, 26], which is a class of Galerkin methods for the approximation of such time-dependent kinetic transport equations. One chooses a set of angular basis functions, tests the kinetic equation against it and integrates over the angular variable, removing the angular dependence while getting a (potentially huge) system of differential equations in space and time. Well-known examples are the classical P_N methods [5, 12, 22], their simplifications, the SP_N [17] methods and entropy minimization M_N models [1, 4, 9, 28, 29]. Especially the latter is favourable since the moment equations are always closed with a positive ansatz function, respecting the positivity of the kinetic distribution to be approximated. In many situations these models perform very well, but since they result from averaging over the complete velocity space, they can produce physically wrong steady-state shocks. It has been shown by Hauck [19] that these shocks exist for every odd order.

To improve this situation, half- or partial-moment models were introduced in [11, 14]. These models work especially well in one space dimension since they capture the potential discontinuity of the probability density in the angular variable which in 1D is well-located. Unfortunately, in a Fokker-Planck operator is used instead of the standard integral-scattering operator (BGK type), these half-moment approximations

fail significantly. A reason for this is that the domain of definition of the Laplace-Beltrami operator requires continuous functions in one dimension. [35].

An intermediate model respecting the continuity of full-moment models while allowing the flexibility of partial moments is the mixed-moment model, which was proposed in [16, 35, 37]. Contrary to a typical half-moment approximation, the lowest order moment (density) is kept as a full moment while all higher moments are half moments.

Although these MM_N models satisfy the above-mentioned property of having a continuous ansatz function, the numerical discretization of it is highly non-trivial due to the appearance of microscopic terms (i.e. the moments of the Laplace-Beltrami operator depend on the values of the ansatz itself). Especially in multiple dimensions, naive implementations fail at discretizing the (semi-)microscopic quantities (line integrals over quadrant/octant boundaries) [34, 37]. To overcome this (numerical) problem, we investigate a modification of the mixed-moment model. This new DMM_N model has more regularity, i.e. its ansatz is differentiable, resulting in a more robust numerical implementation while maintaining most of the benefits of the classical MM_N model.

The first part of the paper shortly reviews the method of moments and the minimum-entropy ansatz. Afterwards, the concept of realizability (the fact, that a moment vector is associated with a non-negative distribution function) is introduced and a concrete characterization of the realizable set for the DMM_2 model is derived. Furthermore, the eigenstructure of this model is explored. Then, the performance of the new model is investigated in two benchmark tests, showing that the DMM_2 is competitive compared to M_N and MM_N models with the same number of degrees of freedom. The paper is concluded by a summary and an outlook on future work.

2. Models

In slab geometry, the transport equation under consideration for the particle distribution $\psi = \psi(t, x, \mu)$ has the form

$$\partial_t \psi + \mu \partial_x \psi + \sigma_a \psi = \sigma_s \mathcal{C}(\psi) + Q, \quad t \in T, x \in X, \mu \in [-1, 1]. \quad (2.1)$$

The physical parameters are the absorption and scattering coefficient $\sigma_a, \sigma_s : T \times X \rightarrow \mathbb{R}_{\geq 0}$, respectively, and the emitting source $Q : T \times X \times [-1, 1] \rightarrow \mathbb{R}_{\geq 0}$.

Collision of particles is modelled by the Laplace-Beltrami operator

$$\mathcal{C}(\psi) = \frac{1}{2} \Delta_\mu \psi = \frac{1}{2} \frac{d}{d\mu} \left((1 - \mu^2) \frac{d\psi}{d\mu} \right).$$

This operator appears, for example, as the result of an asymptotic analysis of the Boltzmann equation under the assumption of small energy loss and deflection, and forward-peaked scattering in the context of electron transport [16, 20, 30].

The transport equation (2.1) is supplemented by initial and boundary conditions:

$$\psi(0, x, \mu) = \psi_{t=0}(x, \mu) \quad \text{for } x \in X = (x_L, x_R), \mu \in [-1, 1], \quad (2.2a)$$

$$\psi(t, x_L, \mu) = \psi_b(t, x_L, \mu) \quad \text{for } t \in T, \mu > 0, \quad (2.2b)$$

$$\psi(t, x_R, \mu) = \psi_b(t, x_R, \mu) \quad \text{for } t \in T, \mu < 0. \quad (2.2c)$$

In general, solving equation (2.1) is very expensive in two and three dimensions due to the high dimensionality of the state space.

For this reason it is convenient to use some type of spectral or Galerkin method to transform the high-dimensional equation into a system of lower-dimensional equations. Typically, one chooses to reduce the dimensionality by representing the angular dependence of ψ in terms of some basis \mathbf{b} .

Definition 2.1. *The vector of functions $\mathbf{b} : [-1, 1] \rightarrow \mathbb{R}^n$ consisting of n basis functions b_i , $i = 0, \dots, n-1$ of maximal order N is called an angular basis.*

The so-called moments of a given distribution function ψ with respect to \mathbf{b} are then defined by

$$\mathbf{u} = \langle \mathbf{b}\psi \rangle = (u_0, \dots, u_{n-1})^T, \quad (2.3)$$

where the integration $\langle \cdot \rangle := \int_{-1}^1 \cdot d\mu$ is performed componentwise.

Assuming for simplicity $b_0 \equiv 1$, the quantity $\rho := u_0 = \langle b_0\psi \rangle = \langle \psi \rangle$ is called local particle density. Furthermore, normalized moments $\phi = (\phi_1, \dots, \phi_{n-1}) \in \mathbb{R}^{n-1}$ are defined as

$$\phi_i = \frac{u_i}{u_0}, \quad i = 1, \dots, n-1. \quad (2.4)$$

To obtain a set of equations for \mathbf{u} , (2.1) has to be multiplied through by \mathbf{b} and integrated over $[-1, 1]$, giving

$$\langle \mathbf{b}\partial_t\psi \rangle + \langle \mathbf{b}\partial_x\mu\psi \rangle + \langle \mathbf{b}\sigma_a\psi \rangle = \sigma_s \langle \mathbf{b}\mathcal{C}(\psi) \rangle + \langle \mathbf{b}Q \rangle.$$

Collecting known terms, and interchanging integrals and differentiation where possible, the moment system has the form

$$\partial_t\mathbf{u} + \partial_x \langle \mu\mathbf{b}\psi \rangle + \sigma_a\mathbf{u} = \sigma_s \langle \mathbf{b}\mathcal{C}(\psi) \rangle + \langle \mathbf{b}Q \rangle. \quad (2.5)$$

The solution of (2.5) is equivalent to the one of (2.1) if \mathbf{b} is a basis of $L_2(\mathcal{S}^2, \mathbb{R})$.

Since it is impractical to work with an infinite-dimensional system, only a finite number of $n < \infty$ basis functions \mathbf{b} of order N can be considered. Unfortunately, there always exists an index $i \in \{0, \dots, n-1\}$ such that the components of $b_i \cdot \mu$ are not in the linear span of \mathbf{b} . Therefore, the flux term cannot be expressed in terms of \mathbf{u} without additional information. Furthermore, the same might be true for the projection of the scattering operator onto the moment-space given by $\langle \mathbf{b}\mathcal{C}(\psi) \rangle$. This is the so-called *closure problem*. One usually prescribes some *ansatz* distribution $\hat{\psi}_{\mathbf{u}}(t, x, \mu) := \hat{\psi}(\mathbf{u}(t, x), \mathbf{b}(\mu))$ to calculate the unknown quantities in (2.5). Note that the dependence on the angular basis in the short-hand notation $\hat{\psi}_{\mathbf{u}}$ is neglected for notational simplicity.

In this paper the ansatz density $\hat{\psi}$ is reconstructed from the moments \mathbf{u} by minimizing the entropy-functional

$$\mathcal{H}(\psi) = \langle \eta(\psi) \rangle \quad (2.6)$$

under the moment constraints

$$\langle \mathbf{b}\psi \rangle = \mathbf{u}. \quad (2.7)$$

The kinetic entropy density $\eta : \mathbb{R} \rightarrow \mathbb{R}$ is strictly convex and twice continuously differentiable and the minimum is simply taken over all functions $\psi = \psi(\mu)$ such that $\mathcal{H}(\psi)$ is well defined. The obtained ansatz $\hat{\psi} = \hat{\psi}_{\mathbf{u}}$, solving this constrained optimization problem, is given by

$$\hat{\psi}_{\mathbf{u}} = \operatorname{argmin}_{\psi: \langle \eta(\psi) \rangle} \{ \langle \eta(\psi) \rangle : \langle \mathbf{b}\psi \rangle = \mathbf{u} \}. \quad (2.8)$$

This problem, which must be solved over the space-time mesh, is typically solved through its strictly convex finite-dimensional dual,

$$\boldsymbol{\alpha}(\mathbf{u}) := \operatorname{argmin}_{\tilde{\boldsymbol{\alpha}} \in \mathbb{R}^n} \left\langle \eta_*(\mathbf{b}^T \tilde{\boldsymbol{\alpha}}) \right\rangle - \mathbf{u}^T \tilde{\boldsymbol{\alpha}}, \quad (2.9)$$

where η_* is the Legendre dual of η . The first-order necessary conditions for the multipliers $\boldsymbol{\alpha}(\mathbf{u})$ show that the solution to (2.8) has the form

$$\hat{\psi}_{\mathbf{u}} = \eta'_* \left(\mathbf{b}^T \boldsymbol{\alpha}(\mathbf{u}) \right), \quad (2.10)$$

where η'_* is the derivative of η_* .

This approach is called the *minimum-entropy closure* [25]. The resulting model has many desirable properties: symmetric hyperbolicity, bounded eigenvalues of the directional flux Jacobian and the direct existence of an entropy-entropy flux pair (compare [25, 34]).

The kinetic entropy density η can be chosen according to the physics being modelled. As in [19, 25], Maxwell-Boltzmann entropy

$$\eta(\psi) = \psi \log(\psi) - \psi \quad (2.11)$$

is used, thus $\eta_*(p) = \eta'_*(p) = \exp(p)$. This entropy is used for non-interacting particles as in an ideal gas.

Substituting ψ in (2.5) with $\hat{\psi}_{\mathbf{u}}$ yields a closed system of equations for \mathbf{u} :

$$\partial_t \mathbf{u} + \partial_x \left\langle \mu \mathbf{b} \hat{\psi}_{\mathbf{u}} \right\rangle + \sigma_a \mathbf{u} = \sigma_s \left\langle \mathbf{b} \mathcal{C} \left(\hat{\psi}_{\mathbf{u}} \right) \right\rangle + \langle \mathbf{b} Q \rangle. \quad (2.12)$$

For convenience, (2.12) can be written in the form of a usual first-order hyperbolic system of balance laws

$$\partial_t \mathbf{u} + \partial_x \mathbf{F}(\mathbf{u}) = \mathbf{s}(\mathbf{u}), \quad (2.13)$$

where

$$\mathbf{F}(\mathbf{u}) = \left\langle \mu \mathbf{b} \hat{\psi}_{\mathbf{u}} \right\rangle \in \mathbb{R}^n, \quad (2.14a)$$

$$\mathbf{s}(\mathbf{u}) = \sigma_s \left\langle \mathbf{b} \mathcal{C} \left(\hat{\psi}_{\mathbf{u}} \right) \right\rangle + \langle \mathbf{b} Q \rangle - \sigma_a \mathbf{u}. \quad (2.14b)$$

In this paper, a variant of the so-called mixed-moment basis [16, 35] is used. This ansatz is a combination of the *full-moment* ($b_i = \mu^i$) and *half-moment monomial basis* ($b_i = \mathbb{1}_{[-1,0]} \mu^i$ or $b_i = \mathbb{1}_{[0,1]} \mu^i$) [10, 11]. The classical mixed-moment basis consists of a full zeroth moment and half moments for every higher moment. The resulting ansatz (2.10) is continuous but not continuously differentiable in $\mu = 0$, leading to a microscopic term of the form $\hat{\psi}_{\mathbf{u}}(0)$ in the scattering term $\left\langle \mathbf{b} \Delta_{\mu} \hat{\psi}_{\mathbf{u}} \right\rangle$ [16, 35]. While this can be treated easily in one dimension, discretization problems arise in higher dimensions, where the microscopic quantity has to be replaced by an integration over a spherical arc of the unit sphere [34, 37].

For this reason, we modify the mixed-moment basis in such a way that the ansatz is differentiable in $\mu = 0$, removing the microscopic quantity. In one dimension, it suffices to choose a full zeroth and first moment to obtain the desired regularity. The corresponding moments have the form

$$\begin{aligned} u_i &= \langle \mu^i \psi \rangle =: \langle b_i \psi \rangle, & i \in \{0, 1\}, \\ u_{i\pm} &= \langle \mu^i \psi \rangle_{\pm} =: \langle b_{i\pm} \psi \rangle, & i \geq 2, \\ \phi_1 &= \frac{u_1}{u_0}, \\ \phi_{i\pm} &= \frac{u_{i\pm}}{u_0}, & i \geq 2, \end{aligned}$$

where $\langle \cdot \rangle_+ = \int_0^1 \cdot d\mu$ and $\langle \cdot \rangle_- = \int_{-1}^0 \cdot d\mu$ denote integration over the halfspaces. Accordingly, the angular basis has the form $\mathbf{b} = (1, \mu, \mathbb{1}_{[0,1]}\mu^2, \dots, \mathbb{1}_{[0,1]}\mu^N, \mathbb{1}_{[-1,0]}\mu^2, \dots, \mathbb{1}_{[-1,0]}\mu^N)^T = (b_0, b_1, b_{2+}, \dots, b_{N+}, b_{2-}, \dots, b_{N-})^T$.

Using this basis, it holds that

$$\begin{aligned} \langle b_0 \Delta_\mu \psi \rangle &= 0, \\ \langle b_1 \Delta_\mu \psi \rangle &= -2u_1, \\ \langle b_{l\pm} \Delta_\mu \psi \rangle &= -l(l+1)u_{l\pm} + l(l-1)u_{(l-2)\pm}, \quad l \in \{2, \dots, N\}. \end{aligned} \quad (2.15)$$

Note that for $l = 2$ and $l = 3$ the quantities $u_{0\pm} = \langle \psi \rangle_\pm$ and $u_{1\pm} = \langle \mu \psi \rangle_\pm$, respectively, appear, which have to be determined using the closure relation (2.10).

Definition 2.2. The *classical mixed-moment model* will be referred to as the MM_N model, while the *differentiable mixed-moment model* will be called the DMM_N model.

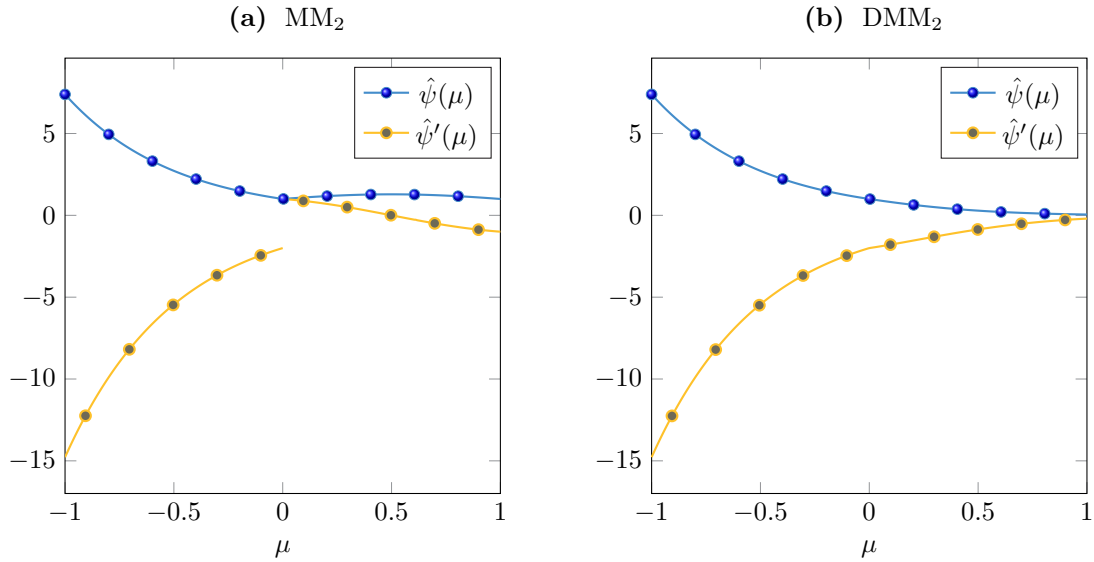


Figure 1: Two ansatz functions and their derivatives for the MM_2 and DMM_2 model, respectively. **Left:** $\hat{\psi}(\mu) = \exp((\mu - \mu^2) \mathbb{1}_{[0,1]} - 2\mu \mathbb{1}_{[-1,0]})$, **Right:** $\hat{\psi}(\mu) = \exp(-2\mu - \mu^2 \mathbb{1}_{[0,1]})$

Figure 1 shows typical ansatz functions $\hat{\psi}$ for the MM_2 and DMM_2 model. It can be seen that the MM_2 ansatz is only continuous, while the DMM_2 ansatz is also continuously differentiable in μ .

3. Realizability

Since the underlying kinetic density to be approximated is non-negative, a moment vector only makes sense physically if it can be associated with a non-negative distribution function. In this case the moment vector is called *realizable*.

Definition 3.1. The realizable set $\mathcal{R}_{\mathbf{b}}$ is

$$\mathcal{R}_{\mathbf{b}} = \{ \mathbf{u} : \exists \psi(\mu) \geq 0, \rho = \langle \psi \rangle > 0, \text{ such that } \mathbf{u} = \langle \mathbf{b} \psi \rangle \}.$$

If $\mathbf{u} \in \mathcal{R}_{\mathbf{b}}$, then \mathbf{u} is called realizable. Any ψ such that $\mathbf{u} = \langle \mathbf{b} \psi \rangle$ is called a representing density.

Remark 3.2.

- (a) The realizable set is a convex cone, and
- (b) Representing densities are not necessarily unique.

Additionally, since the entropy ansatz has the form (2.10), in the Maxwell-Boltzmann case, the optimization problem (2.8) only has a solution if the moment vector lies in the ansatz space

$$\mathcal{A} := \left\{ \left\langle \mathbf{b} \hat{\psi}_{\mathbf{u}} \right\rangle \stackrel{(2.10)}{=} \left\langle \mathbf{b} \eta'_* \left(\mathbf{b}^T \boldsymbol{\alpha} \right) \right\rangle : \boldsymbol{\alpha} \in \mathbb{R}^n \right\}.$$

In the case of a bounded angular domain, the ansatz space \mathcal{A} is equal to the set of realizable moment vectors [23]. Therefore, it is sufficient to focus on realizable moments only.

Unfortunately, the definition of the realizable set is not constructive, making it hard to check if a moment vector is realizable or not. Therefore, other characterizations of $\mathcal{R}_{\mathbf{b}}$ are necessary.

For example, in the classical mixed-moment problem of first order, the realizable set is characterized by the inequalities [16, 35]

$$u_{1+} - u_{1-} \leq u_0 \quad \text{and} \quad \pm u_{1\pm} \geq 0.$$

In this paper, we want to focus on the lowest-order non-trivial model of the differentiable mixed-moment hierarchy, i.e. $N = 2$.

Theorem 3.3. *The moment vector $\mathbf{u} = (u_0, u_1, u_{2+}, u_{2-}) \in \mathbb{R}^4$ is realizable, i.e. $\mathbf{u} \in \mathcal{R}_{\mathbf{b}}$, if and only if*

$$u_{2+} - \sqrt{u_{2-} (u_0 - u_{2+})} \leq u_1 \leq \sqrt{u_{2+} (u_0 - u_{2-})} - u_{2-}, \quad (3.1)$$

$$u_0, u_{2\pm} \geq 0. \quad (3.2)$$

Proof. At first, we want to show that (3.1) and (3.2) are necessary. Assume that $\psi \geq 0$ is arbitrary but fixed and $\mathbf{u} = \langle \mathbf{b} \psi \rangle$. Note that $u_{0\pm} \geq \pm u_{1\pm} \geq u_{2\pm} \geq 0$ and $u_{0\pm} u_{2\pm} \geq u_{1\pm}^2$ due to the half-moment realizability conditions [8, 35]. Then we have (using $u_{0-} + u_{0+} = u_0$) that

$$u_{2-} (u_0 - u_{2+}) = u_{2-} u_{0-} + u_{2-} (u_{0+} - u_{2+}) \geq u_{1-}^2 + u_{2-} (u_{0+} - u_{2+}) \geq u_{1-}^2.$$

Since $u_{1-} \leq 0$ it follows that

$$\sqrt{u_{2-} (u_0 - u_{2+})} \geq |u_{1-}| = -u_{1-} \quad \iff \quad -\sqrt{u_{2-} (u_0 - u_{2+})} \leq u_{1-}.$$

Therefore

$$u_{2+} - \sqrt{u_{2-} (u_0 - u_{2+})} \leq u_{2+} + u_{1-} \leq u_{1+} + u_{1-} = u_1.$$

The upper bound can be shown to be necessary in a similar way.

(3.2) follows from the positivity of 1 and μ^2 . We want to remark that the standard second-order full-moment realizability condition for $u_2 = u_{2+} + u_{2-}$, namely $u_0 (u_{2+} + u_{2-}) \geq u_1^2$, is implied by (3.1) and (3.2).

To show that the above inequalities are also sufficient, we provide a non-negative realizing distribution with support in $[-1, 1]$:

$$\psi = u_0 \left(\frac{\phi_{1+}^2}{\phi_{2+}} \cdot \delta \left(\mu - \frac{\phi_{2+}}{\phi_{1+}} \right) + \frac{\phi_{1-}^2}{\phi_{2-}} \cdot \delta \left(\mu - \frac{\phi_{2-}}{\phi_{1-}} \right) \right),$$

with

$$\phi_{1+} = \frac{\phi_{2+} \left(\phi_1 + \phi_{2-} \sqrt{\frac{-\phi_1^2 + \phi_{2-} + \phi_{2+}}{\phi_{2-} \phi_{2+}}} \right)}{\phi_{2-} + \phi_{2+}}$$

$$\phi_{1-} = \frac{\phi_{2-} \left(\phi_1 - \phi_{2+} \sqrt{\frac{-\phi_1^2 + \phi_{2-} + \phi_{2+}}{\phi_{2-} \phi_{2+}}} \right)}{\phi_{2-} + \phi_{2+}}$$

and $\phi_{1+} = \phi_{1-} = 0$ if $\phi_{2+} = \phi_{2-} = 0$. In this case, $\psi = u_0 \delta(\mu)$ (due to the quadratic term the second moment vanishes faster than the first moment so we have $\frac{\phi_{2\pm}}{\phi_{1\pm}} \rightarrow 0$ and $\frac{\phi_{1\pm}^2}{\phi_{2\pm}} \rightarrow \frac{\phi_{2\mp} - \phi_1^2}{\phi_{2\mp}}$). It is simple to check that $\phi_{1+} + \phi_{1-} = \phi_1$ and $\frac{\phi_{1+}^2}{\phi_{2+}} + \frac{\phi_{1-}^2}{\phi_{2-}} = 1$, i.e. all moments are correctly represented. It remains to show that under (3.1) we have that $\frac{\phi_{2+}}{\phi_{1+}} \in [0, 1]$ and $\frac{\phi_{2-}}{\phi_{1-}} \in [-1, 0]$, i.e.

$$0 \leq \phi_{2\pm} \leq \pm \phi_{1\pm}.$$

This corresponds to the standard half-moment realizability conditions of second order. We first note that (3.1) and (3.2) imply that $\phi_{2\pm} \in [0, 1]$ since otherwise the bounds become complex. Second, we have that $\phi_{2+} - \sqrt{\phi_{2-} (1 - \phi_{2+})} = \sqrt{\phi_{2+} (1 - \phi_{2-})} - \phi_{2-}$ if and only if $\phi_{2+} = 1 - \phi_{2-}$ or $\phi_{2+} = \phi_{2-} = 0$, implying the classical full-moment realizability conditions $\phi_1 \in [-1, 1]$ and $\phi_2 \leq 1$.

We start the investigation at the different parts of the realizability boundary.

Let $\phi_1 = \sqrt{\phi_{2+} (1 - \phi_{2-})} - \phi_{2-}$. Plugging this into the definition of ϕ_{1+} we get that, after some elementary transformations,

$$\begin{aligned} \phi_{1+} &\geq \frac{\phi_{2+}}{\phi_{2+} + \phi_{2-}} \left(\sqrt{1 - \phi_{2-}} \left(\sqrt{\phi_{2+}} + \frac{\phi_{2-}}{\sqrt{\phi_{2+}}} \right) \right) \\ &\stackrel{1 \geq \phi_{2+} + \phi_{2-}}{\geq} \frac{\phi_{2+}}{\phi_{2+} + \phi_{2-}} \left(\sqrt{\phi_{2+}} \left(\sqrt{\phi_{2+}} + \frac{\phi_{2-}}{\sqrt{\phi_{2+}}} \right) \right) = \phi_{2+}. \end{aligned}$$

Similarly, we obtain $-\phi_{1-} \geq \phi_{2-}$ and the same in the case $\phi_1 = \phi_{2+} - \sqrt{\phi_{2-} (1 - \phi_{2+})}$.

Since the realizable set is always convex, the argumentation must also hold in the interior of the above set. \square

The *normalized realizable set*

$$\mathcal{R}_{\mathbf{b}}|_{\rho=1} = \{\mathbf{u} \in \mathcal{R}_{\mathbf{b}} \mid \rho = 1\}$$

of the DMM₂ model, defined by (3.1) and (3.2), is shown in Figure 2.

Remark 3.4. (3.1) gives a surprising insight into realizability of mixed-moment models. While the realizable set for full-moment and classical mixed-moment models can be characterized by inequalities with rational functions of the moments, the differential mixed-moment model requires non-linearities. This implies that it might be impossible to transfer the general mixed-moment structure (which uses a linearity argument) shown in [35] to the differentiable case.

4. Eigenstructure of the DMM₂ model

It is well known that the moment system (2.12) admits desirable properties like symmetric hyperbolicity, boundedness of the characteristic velocities (eigenvalues of the flux Jacobian) and the existence of an entropy-entropy flux pair [2, 25, 26, 34]. Furthermore, the eigenvalues only depend on the normalized moments ϕ .

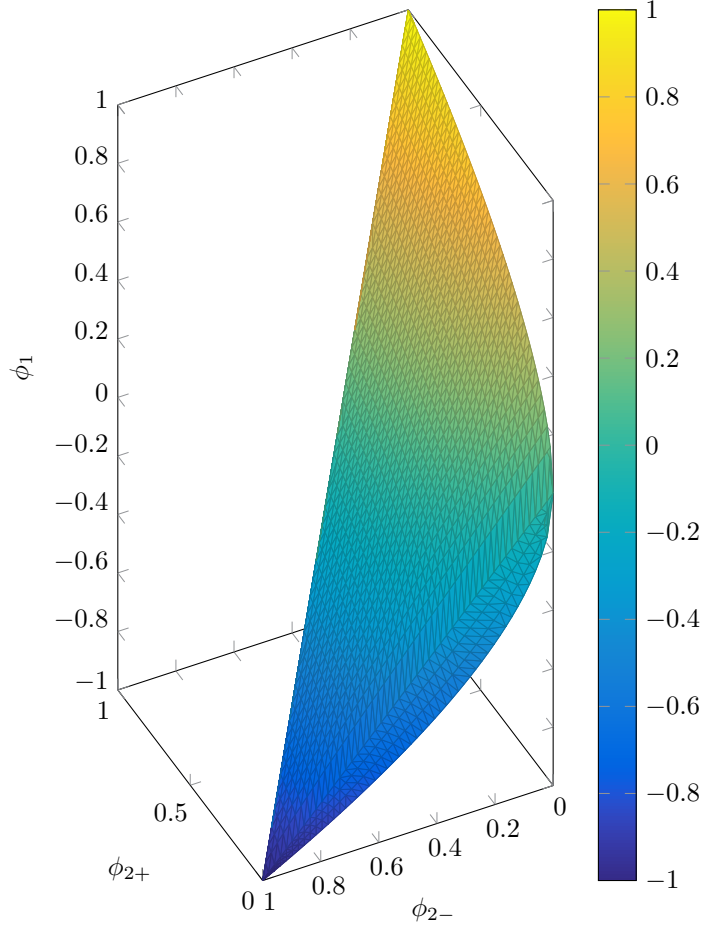


Figure 2: The normalized realizable set for the differentiable mixed-moment basis of order $N = 2$.
Online version: Press to activate 3D view (x -axis (red): ϕ_{2+} , y -axis (green): ϕ_{2-} , z -axis (blue): ϕ_1)

If we define $\mathbf{J}(\boldsymbol{\alpha}) := \langle \mu \mathbf{b} \mathbf{b}^T \eta_*''(\mathbf{b}^T \boldsymbol{\alpha}) \rangle$ and $\mathbf{H}(\boldsymbol{\alpha}) := \langle \mathbf{b} \mathbf{b}^T \eta_*''(\mathbf{b}^T \boldsymbol{\alpha}) \rangle$, the flux Jacobian of (2.13) has the form [2, 25, 34]

$$\frac{\partial \mathbf{F}(\mathbf{u})}{\partial \mathbf{u}} = \mathbf{J}(\boldsymbol{\alpha}(\mathbf{u})) \frac{\partial \boldsymbol{\alpha}(\mathbf{u})}{\partial \mathbf{u}} = \mathbf{J}(\boldsymbol{\alpha}(\mathbf{u})) \mathbf{H}(\boldsymbol{\alpha}(\mathbf{u}))^{-1}. \quad (4.1)$$

In the special case of the DMM_2 model, the flux Jacobian is given by

$$\frac{\partial \mathbf{F}(\mathbf{u})}{\partial \mathbf{u}} = \begin{pmatrix} 0 & 1 & 0 & 0 \\ 0 & 0 & 1 & 1 \\ \frac{\partial u_{3+}}{\partial \mathbf{u}} \\ \frac{\partial u_{3-}}{\partial \mathbf{u}} \end{pmatrix}, \quad (4.2)$$

where $u_{3\pm} = \langle \mu^3 \hat{\psi}_{\mathbf{u}} \rangle_{\pm}$ is obtained via the closure relation.

The four eigenvalues $\lambda_1 \leq \lambda_2 \leq \lambda_3 \leq \lambda_4$ of (4.2), which have been obtained numerically, are shown in Figures 3 to 6. In Figure 3, the eigenvalues are shown along the cut

$$\phi_1 = \frac{1}{2} \left(\phi_{2+} - \sqrt{\phi_{2-} (1 - \phi_{2+})} + \sqrt{\phi_{2+} (1 - \phi_{2-})} - \phi_{2-} \right),$$

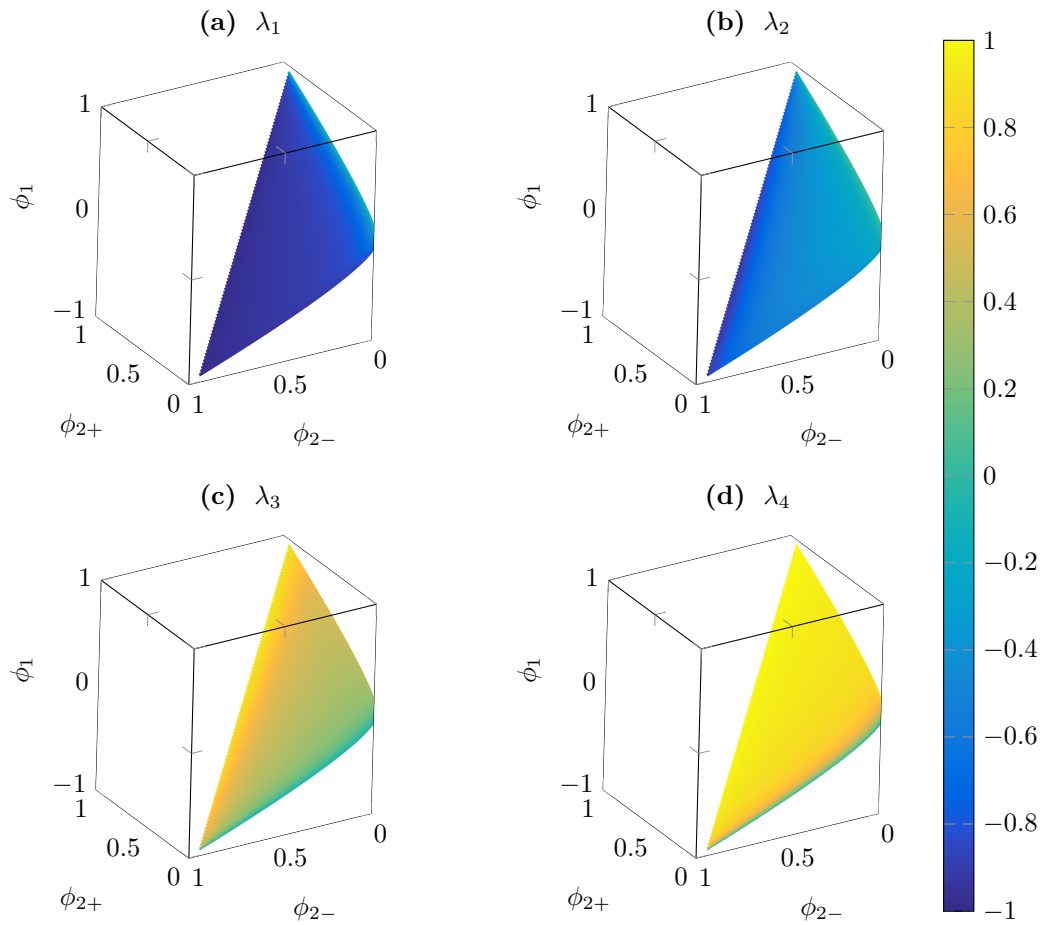


Figure 3: Eigenvalues of the DMM₂ flux Jacobian $\frac{\partial \mathbf{F}(\mathbf{u})}{\partial \mathbf{u}}$ along $\phi_1 = \frac{1}{2} \left(\phi_{2+} - \sqrt{\phi_{2-}(1-\phi_{2+})} + \sqrt{\phi_{2+}(1-\phi_{2-})} - \phi_{2-} \right)$.

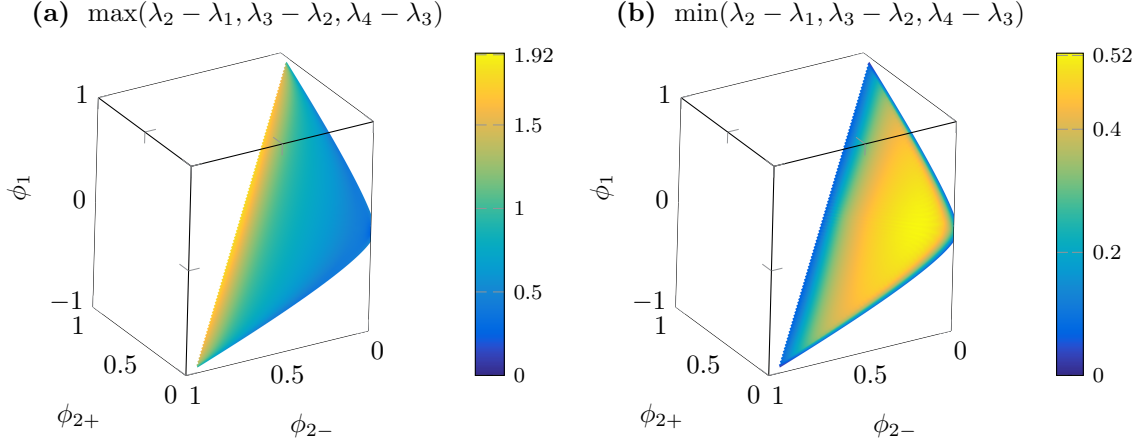


Figure 4: Minimal and maximal distance between adjacent eigenvalues of the DMM₂ flux Jacobian $\frac{\partial \mathbf{F}(\mathbf{u})}{\partial \mathbf{u}}$ along the cut $\phi_1 = \frac{1}{2} \left(\phi_{2+} - \sqrt{\phi_{2-}(1-\phi_{2+})} + \sqrt{\phi_{2+}(1-\phi_{2-})} - \phi_{2-} \right)$.

which is exactly the mean of the upper and lower bound on ϕ_1 .

It can be seen that the eigenvalues are discontinuous in the degenerate corners of the realizable set (e.g. λ_4 at $\phi_{2-} = 1 = -\phi_1$, $\phi_{2+} = 0$). This property exists also for the classical mixed-moment MM₁ or the M₂ model [34].

We investigate the hyperbolicity of the moment system in Figure 4 by comparing the distances of adjacent eigenvalues. Figure 4a shows that all eigenvalues coincide only if $\phi_1 = \phi_{2+} = \phi_{2-} = 0$. Otherwise, at least two eigenvalues differ from each other.

The results in Figure 4b propose the strict hyperbolicity of the moment system in the interior of the realizable set (since all eigenvalues differ). However, at the realizability boundary (e.g. $\phi_{2+} + \phi_{2-} = 1$) at least two eigenvalues coincide.

Since the optimization problem (2.9) is ill-conditioned close to the realizability boundary, the calculation of the multipliers α at this part of the realizable set is error-prone or impossible, resulting in meaningless pictures. We therefore investigate **isotropically-regularized moments**

$$\phi_r = (1-r)\phi + r\phi_{\text{iso}},$$

where an increase of the regularization parameter $r \in [0, 1]$ moves the original moment vector ϕ towards the isotropic moment vector (in case of the DMM₂ model: $\phi_{\text{iso}} = (0, \frac{1}{6}, \frac{1}{6})^T$). Figure 5 shows the eigenvalues for $r = 0.05$ and $\phi \in \partial \mathcal{R}_{\mathbf{b}}|_{\rho=1}$.

Similar to Figure 4b, Figure 6 shows the minimal distance of the 5% regularized boundary moments. It is visible that the minimal distance is attained at $\phi_{2+} + \phi_{2-} = 1$, which indicates that on this part of the boundary the moment system is only weakly hyperbolic.

However, an analytical investigation of the eigenvalues in the limit cases $\phi_1 = \phi_{2+} - \sqrt{\phi_{2-}(1-\phi_{2+})}$ and $\phi_1 = \sqrt{\phi_{2+}(1-\phi_{2-})} - \phi_{2-}$ is still open.

5. Numerical experiments

We use the first-order, realizability-preserving, implicit-explicit kinetic scheme derived in [31]. All results are computed on a grid with 1000 points. The reference solution is given by the P₉₉ model [27].

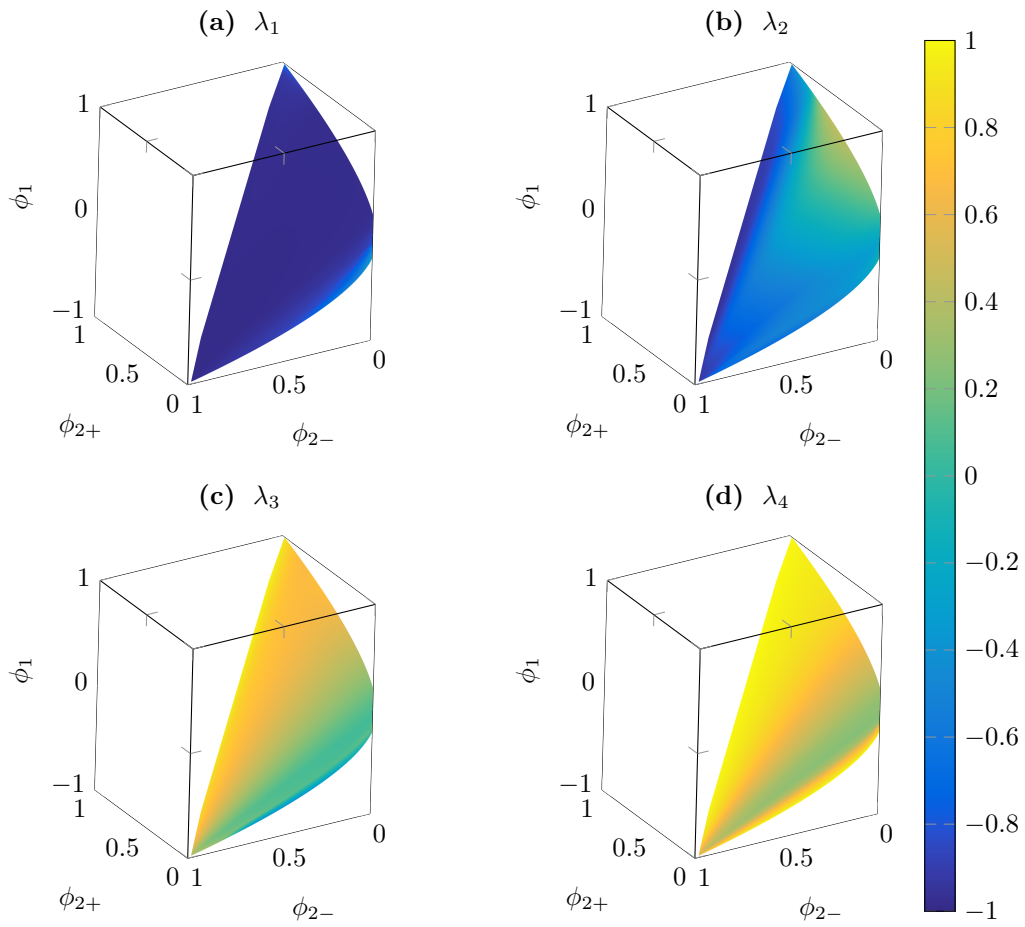


Figure 5: Eigenvalues at 5% regularized boundary moments.

Online version: Press to activate 3D view (x -axis (red): ϕ_{2+} , y -axis (green): ϕ_{2-} , z -axis (blue): ϕ_1)

(a) $\min(\lambda_2 - \lambda_1, \lambda_3 - \lambda_2, \lambda_4 - \lambda_3)$

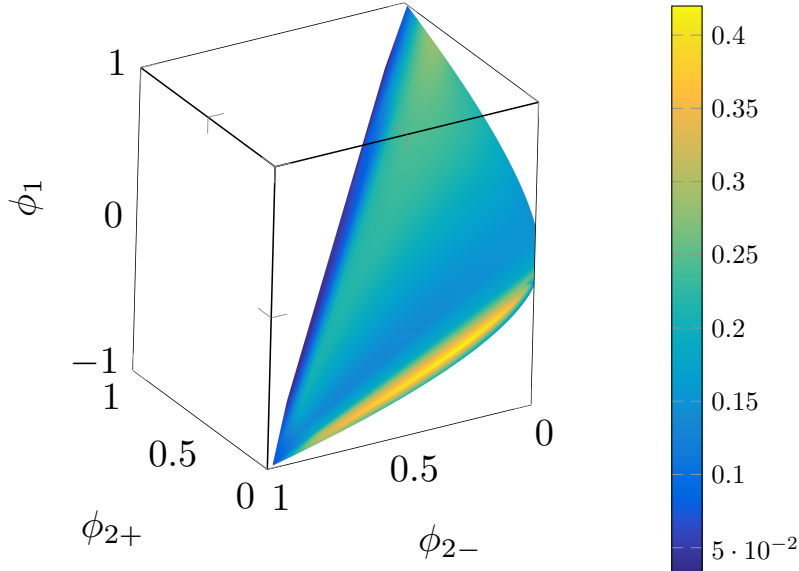


Figure 6: Minimal eigenvalue distance for 5% regularized boundary moments.

Online version: Press to activate 3D view (x -axis (red): ϕ_{2+} , y -axis (green): ϕ_{2-} , z -axis (blue): ϕ_1)

5.1. Plane source

In this test case an isotropic distribution with all mass concentrated in the middle of an infinite domain $x \in (-\infty, \infty)$ is defined as initial condition, i.e.

$$\psi_{t=0}(x, \mu) = \psi_{\text{vac}} + \delta(x),$$

where the small parameter $\psi_{\text{vac}} = 0.5 \times 10^{-8}$ is used to approximate a vacuum. In practice, a bounded domain must be used which is large enough that the boundary should have only negligible effects on the solution. For the final time $t_f = 1$, the domain is set to $X = [-1.2, 1.2]$ (recall that for all presented models the maximal speed of propagation is bounded in absolute value by one).

At the boundary the vacuum approximation

$$\psi_b(t, x_L, \mu) \equiv \psi_{\text{vac}} \quad \text{and} \quad \psi_b(t, x_R, \mu) \equiv \psi_{\text{vac}}$$

is used again. Furthermore, the physical coefficients are set to $\sigma_s \equiv 1$, $\sigma_a \equiv 0$ and $Q \equiv 0$.

All solutions are computed with an even number of cells, so the initial Dirac delta lies on a cell boundary. Therefore it is approximated by splitting it into the cells immediately to the left and right. In Figure 7, only positive x are shown since the solutions are always symmetric around $x = 0$.

The figure shows the solution of the DMM_2 model in comparison to some mixed-moment MM_N and full-moment M_N models with a similar number of degrees of freedom (i.e. the number of moments n).

Observe that the difference between MM_2 and DMM_2 is negligible¹. Although the DMM_2 model is exactly

¹This is no longer true if the isotropic scattering operator $\mathcal{C}(\psi) = \psi - \frac{1}{2} \int_{-1}^1 \psi(\mu') d\mu'$ is used.

between MM_1 and MM_2 (regarding degrees of freedom), its solution is much closer to those of the MM_2 model.

Doing the same comparison with the M_N models shows that the DMM_2 model is closer to the M_2 than to the M_3 model (while all three models differ insignificantly from the reference solution²).

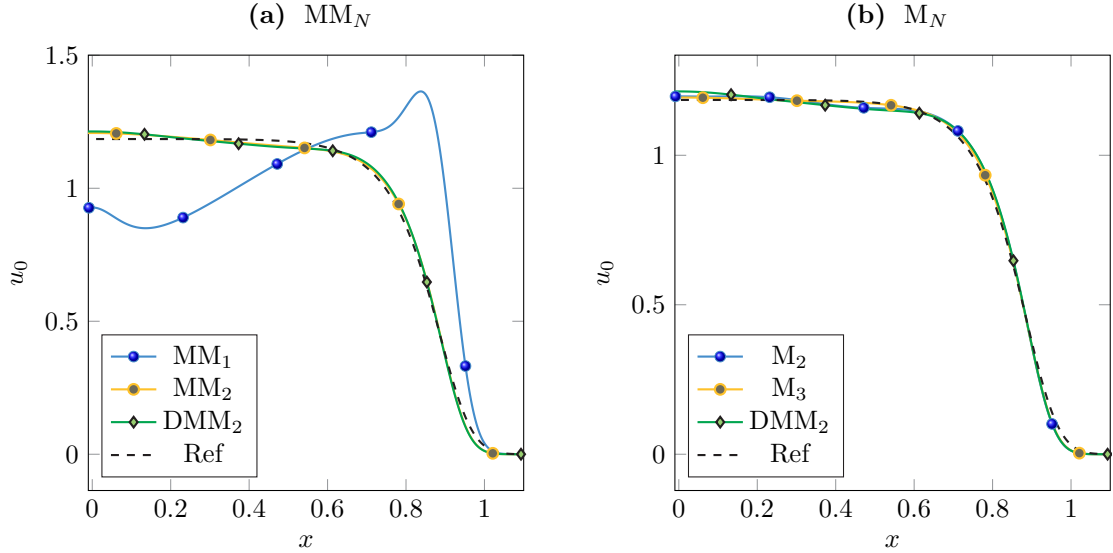


Figure 7: Results for the plane-source test at the final time $t_f = 1$.

5.2. Source beam

We present a discontinuous version of the source-beam problem from [15], as in [2, 36]. The spatial domain is $X = [0, 3]$, and

$$\sigma_a(x) = \begin{cases} 1 & \text{if } x \leq 2, \\ 0 & \text{else,} \end{cases} \quad \sigma_s(x) = \begin{cases} 0 & \text{if } x \leq 1, \\ 2 & \text{if } 1 < x \leq 2, \\ 10 & \text{else,} \end{cases} \quad Q(x) = \begin{cases} \frac{1}{2} & \text{if } 1 \leq x \leq 1.5, \\ 0 & \text{else,} \end{cases}$$

with initial and boundary conditions

$$\psi_{t=0}(x, \mu) \equiv \psi_{\text{vac}},$$

$$\psi_b(t, x_L, \mu) = \frac{e^{-10^5(\mu-1)^2}}{\langle e^{-10^5(\mu-1)^2} \rangle} \quad \text{and} \quad \psi_b(t, x_R, \mu) \equiv \psi_{\text{vac}}.$$

The final time is $t_f = 2.5$. As above, the results for M_N , MM_N and DMM_N models are shown in Figure 8.

As has been remarked in [34], the MM_1 and the M_2 model coincide well in this situation. Surprisingly, a similar statement is valid for the DMM_2 and M_3 model. As before, the DMM_2 model behaves qualitatively above the level of the MM_1 and M_2 model and similarly or slightly below those of the MM_2 model (which has the highest number of degrees of freedom).

²This results from the quadratic dependence of the Laplace-Beltrami eigenvalues with respect to the moment order N .

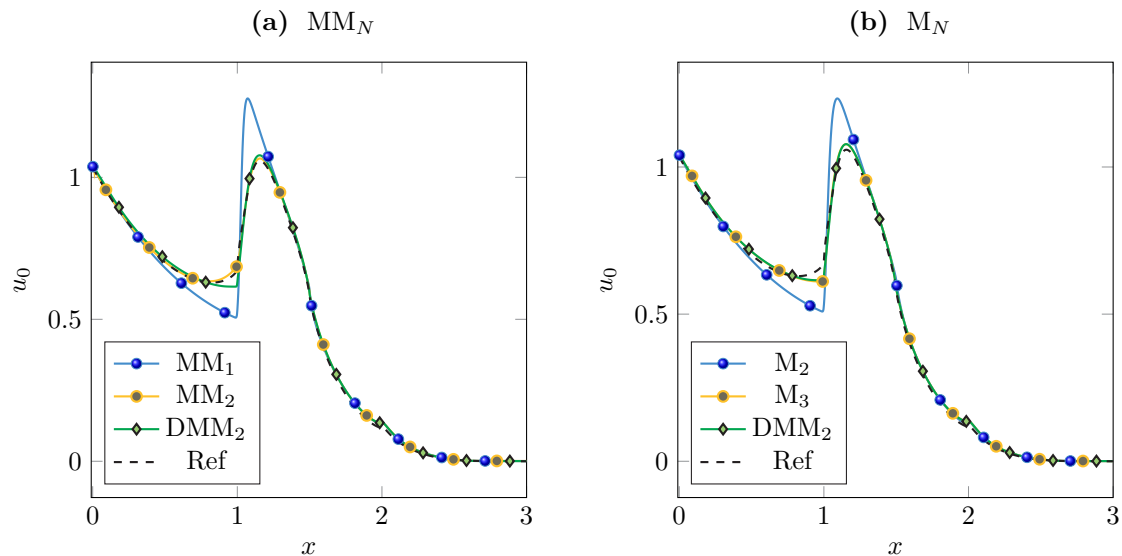


Figure 8: Results for the source-beam test at the final time $t_f = 2.5$.

6. Conclusions and outlook

We have derived the DMM_N model and its associated realizability domain $\mathcal{R}_{\mathbf{b}}$ for $N = 2$. Numerical results suggest that, despite having one degree of freedom less, the DMM_2 model performs comparable to the MM_2 model. The key advantage of this class of moment models is that in the approximation of the Laplace-Beltrami operator only macroscopic quantities occur, whereas microscopic terms are present in the classical mixed-moment model. While this appears to have no significant impact in one dimension, where the position of the microscopic term is well-located, a more stable numerical approximation can be expected in two or three dimensions.

Future work should include the derivation of realizability theory for moment-orders $N \geq 3$, to gain more insight into the arising non-linearities in this modified problem. Furthermore, the DMM_N should be investigated in higher dimensions, especially in the context of the Fokker-Planck operator. The results in [34, 37] indicate that mixed moments are hardly applicable in this framework due to the difficulty in the discretization of the Laplace-Beltrami operator. This should be avoidable using the differentiable basis functions. Finally, Kershaw closures [24, 32, 33, 35] should be investigated to improve the efficiency of the DMM_N model by avoiding the need to solve the moment system (2.7).

Acknowledgements

The conversion from Matlab data to the included u3d data has been obtained using the Matlab function `fig2u3d` written by Ioannis Filippidis [13].

References

- [1] G. W. ALLDREDGE, C. D. HAUCK, AND A. L. TITS, *High-Order Entropy-Based Closures for Linear Transport in Slab Geometry II: A Computational Study of the Optimization Problem*, SIAM Journal on Scientific Computing, 34 (2012), pp. B361–B391.
- [2] G. W. ALLDREDGE AND F. SCHNEIDER, *A realizability-preserving discontinuous Galerkin scheme for entropy-based moment closures for linear kinetic equations in one space dimension*, Journal of Computational Physics, 295 (2015), pp. 665–684.

- [3] L. BOLTZMANN, *Weitere Studien über das Wärmegleichgewicht unter Gasmolekülen*, Wien. Ber., 66 (1872), pp. 275–370.
- [4] T. A. BRUNNER AND J. P. HOLLOWAY, *One-dimensional Riemann solvers and the maximum entropy closure*, Journal of Quantitative Spectroscopy and Radiative Transfer, 69 (2001), pp. 543–566.
- [5] ———, *Two-dimensional time dependent Riemann solvers for neutron transport*, Journal of Computational Physics, 210 (2005), pp. 386–399.
- [6] C. CERCIGNANI, *The Boltzmann Equation and Its Applications*, Applied Mathematical Sciences, Springer New York, 2012.
- [7] F. CHALUB AND P. MARKOWICH, *Kinetic models for chemotaxis and their drift-diffusion limits*, Springer Vienna, Vienna, 2004.
- [8] R. CURTO AND L. FIALKOW, *Recursiveness, positivity, and truncated moment problems*, Houston J. Math, 17 (1991), pp. 603–636.
- [9] B. DUBROCA AND J.-L. FEUGEAS, *Entropic Moment Closure Hierarchy for the Radiative Transfer Equation*, C. R. Acad. Sci. Paris Ser. I, 329 (1999), pp. 915–920.
- [10] B. DUBROCA, M. FRANK, A. KLAR, AND G. THÖMMES, *Half space moment approximation to the radiative heat transfer equations*, ZAMM - Journal of Applied Mathematics and Mechanics / Zeitschrift für Angewandte Mathematik und Mechanik, 83 (2003), pp. 853–858.
- [11] B. DUBROCA AND A. KLAR, *Half-Moment Closure for Radiative Transfer Equations*, Journal of Computational Physics, 180 (2002), pp. 584–596.
- [12] A. S. EDDINGTON, *The Internal Constitution of the Stars*, Dover, 1926.
- [13] I. FILIPPIDIS, *fig2u3d*, <https://de.mathworks.com/matlabcentral/fileexchange/37640-export-figure-to-3d-interactive-pdf>, (2015).
- [14] M. FRANK, B. DUBROCA, AND A. KLAR, *Partial moment entropy approximation to radiative heat transfer*, Journal of Computational Physics, 218 (2006), pp. 1–18.
- [15] M. FRANK, C. HAUCK, AND E. OLBRANT, *Perturbed, entropy-based closure for radiative transfer*, Kinetic and Related Models, 6 (2013), pp. 557–587.
- [16] M. FRANK, H. HENSEL, AND A. KLAR, *A fast and accurate moment method for the Fokker-Planck equation and applications to electron radiotherapy*, SIAM Journal on Applied Mathematics, 67 (2007), pp. 582–603.
- [17] E. M. GELBARD, *Simplified spherical harmonics equations and their use in shielding problems*, Tech. Rep. WAPD-T-1182, Bettis Atomic Power Laboratory, 1961.
- [18] K. P. HADELER, *Reaction transport equations in biological modeling*, in Mathematical and Computer Modelling, vol. 31, 2000, pp. 75–81.
- [19] C. D. HAUCK, *High-order entropy-based closures for linear transport in slab geometry*, Communications in Mathematical Sciences, 9 (2011), pp. 187–205.
- [20] H. HENSEL, R. IZA-TERAN, AND N. SIEDOW, *Deterministic model for dose calculation in photon radiotherapy*, Physics in medicine and biology, 51 (2006), pp. 675–693.
- [21] T. HILLEN AND K. J. PAINTER, *Transport and anisotropic diffusion models for movement in oriented habitats*, Lecture Notes in Mathematics, 2071 (2013), pp. 177–222.
- [22] J. H. JEANS, *The equations of radiative transfer of energy*, Monthly Notices Royal Astronomical Society, 78 (1917), pp. 28–36.
- [23] M. JUNK, *Maximum entropy for reduced moment problems*, Math. Meth. Mod. Appl. Sci., 10 (2000), pp. 1001–1025.
- [24] D. S. KERSHAW, *Flux Limiting Nature’s Own Way: A New Method for Numerical Solution of the Transport Equation*, Lawrence Livermore National Laboratory, UCRL-78378, (1976).
- [25] C. D. LEVERMORE, *Moment closure hierarchies for kinetic theories*, Journal of Statistical Physics, 83 (1996), pp. 1021–1065.
- [26] ———, *Moment Closure Hierarchies for the Boltzmann-Poisson Equation*, VLSI Design, 6 (1998), pp. 97–101.
- [27] E. E. LEWIS AND J. W. F. MILLER, *Computational Methods in Neutron Transport*, John Wiley and Sons, New York, 1984.
- [28] G. N. MINERBO, *Maximum entropy Eddington factors*, J. Quant. Spectrosc. Radiat. Transfer, 20 (1978), pp. 541–545.
- [29] P. MONREAL AND M. FRANK, *Higher order minimum entropy approximations in radiative transfer*, arXiv preprint arXiv:0812.3063, (2008), pp. 1–18.
- [30] G. C. POMRANING, *The Fokker-Planck operator as an asymptotic limit*, Math. Mod. Meth. Appl. Sci., 2 (1992), pp. 21–36.
- [31] F. SCHNEIDER, *Implicit-explicit, realizability-preserving first-order scheme for moment models with Lipschitz-continuous source terms*, arXiv preprint, (2016).
- [32] ———, *Kershaw closures for linear transport equations in slab geometry I: Model derivation*, Journal of Computational Physics, 322 (2016), pp. 905–919.
- [33] ———, *Kershaw closures for linear transport equations in slab geometry II: high-order realizability-preserving discontinuous-Galerkin schemes*, Journal of Computational Physics, 322 (2016), pp. 920–935.
- [34] ———, *Moment models in radiation transport equations*, Dr. Hut Verlag, mathematik ed., 2016.
- [35] F. SCHNEIDER, G. W. ALLDREDGE, M. FRANK, AND A. KLAR, *Higher Order Mixed-Moment Approximations for the Fokker-Planck Equation in One Space Dimension*, SIAM Journal on Applied Mathematics, 74 (2014), pp. 1087–1114.
- [36] F. SCHNEIDER, J. KALL, AND G. ALLDREDGE, *A realizability-preserving high-order kinetic scheme using WENO reconstruction for entropy-based moment closures of linear kinetic equations in slab geometry*, Kinetic and Related Models, 9 (2015), pp. 193–215.
- [37] F. SCHNEIDER, J. KALL, AND A. ROTH, *First-order quarter- and mixed-moment realizability theory and Kershaw closures for a Fokker-Planck equation in two space dimensions*, Kinetic and Related Models, to appear (2016).